

Static and fluctuating stripe order observed by resonant soft x-ray diffraction in $\text{La}_{1.8}\text{Sr}_{0.2}\text{NiO}_4$

J. Schlappa,¹ C. F. Chang,¹ E. Schierle,^{2,3} A. Tanaka,⁴ R. Feyerherm,³ Z. Hu,¹ H. Ott,¹ O. Friedt,^{1,5} E. Dudzik,³ H.-H. Hung,⁶ M. Benomar,¹ M. Braden,¹ L. H. Tjeng,¹ and C. Schüßler-Langeheine^{1,*}

¹*II. Physikalisches Institut, Universität zu Köln, Zùlpicher Str. 77, D-50937 Köln, Germany*

²*Institut für Experimentalphysik, Freie Universität Berlin, Arnimallee 14, D-14195 Berlin, Germany*

³*Helmholtz Centre Berlin for Materials and Energy, Albert-Einstein-Str. 15, 12489 Berlin, Germany*

⁴*Department of Quantum Matter, ADSM, Hiroshima University, Higashi-Hiroshima 739-8530, Japan*

⁵*Laboratoire Léon Brillouin, CEA-Saclay, 91191 Gif-sur-Yvette Cedex, France*

⁶*National Hsinchu University of Education, Hsinchu, Taiwan*

(Dated: February 3, 2022)

We studied the stripe phase of $\text{La}_{1.8}\text{Sr}_{0.2}\text{NiO}_4$ using neutron diffraction, resonant soft x-ray diffraction (RSXD) at the Ni $L_{2,3}$ edges, and resonant x-ray diffraction (RXD) at the Ni K threshold. Differences in the q -space resolution of the different techniques have to be taken into account for a proper evaluation of diffraction intensities associated with the spin and charge order superstructures. We find that in the RSXD experiment the spin and charge order peaks show the same temperature dependence. In the neutron experiment by contrast, the spin and charge signals follow quite different temperature behaviors. We infer that fluctuating magnetic order contributes considerably to the magnetic RSXD signal and we suggest that this result may open an interesting experimental approach to search for fluctuating order in other systems by comparing RSXD and neutron diffraction data.

PACS numbers: 71.27.+a, 71.45.Lr, 75.50.Ee, 61.10.Dp

Sr-doped La_2NiO_4 (LSNO) and La_2CuO_4 (LSCO) form at low temperatures an ordered phase of charge and spin degrees of freedom, the so called stripes. This phase consists of one-dimensional hole rich lines, which form antiphase domain walls for the antiferromagnetic background of the hole-poor regions.^{1,2,3} The stripe phase has attracted considerable interest because of its possible relation to cuprate superconductivity.⁴ While in LSNO static stripe order is found at low temperatures, LSCO exhibits fluctuating stripe order which can be rendered static by additional doping.⁵ From neutron diffraction it is known that in LSNO static spin order (SO) sets in at a Néel temperature T_N well below the charge ordering (CO) temperature T_{CO} .^{6,7,8,9,10} Yet, above T_N , fluctuating magnetic correlations can be found at finite energies.^{11,12}

Most experimental results concerning the structure of the stripe phase are based on neutron diffraction experiments, which are sensitive to magnetic order and to the lattice distortion caused by the charge ordering. In a neutron scattering experiment one can readily distinguish between static and fluctuating magnetic ordering by energy analysis of the scattered neutrons. Static order yields an elastic signal, while magnetic fluctuations lead to a finite energy change of the scattered neutrons.

Recently resonant soft x-ray diffraction (RSXD) has been shown to be another powerful experimental tool to study stripes or similar order phenomena, because of its high sensitivity to spatial modulations of the electronic state and its high magnetic scattering contrast^{13,14,15,16,17}. It is therefore well suited to study both the charge and the magnetic signal from a stripe

system. We have used RSXD before to identify the *electronic* character of the stripe phase in $\text{La}_{1.8}\text{Sr}_{0.2}\text{NiO}_4$.¹⁷ Now we would like to address the question of the temperature dependence of SO and CO in this system. Earlier conventional x-rays experiments from CO in LSNO found an interesting discrepancy to the neutron findings for the low temperature behavior: while the neutron CO signal increases monotonically upon cooling and eventually saturates,^{6,7,8,10,12,18} conventional x-rays found a maximum intensity at intermediate temperatures and a decay of the CO signal upon cooling.^{19,20,21,22,23} This effect has been discussed in terms of a surface effect or of a difference in the signals probed by neutron and x-ray diffraction,²³ but no conclusive explanation has been given so far.

Here we carried out a comprehensive study on $\text{La}_{1.8}\text{Sr}_{0.2}\text{NiO}_4$ in which we compare the temperature dependence of the SO and CO signals, and in which we use neutron diffraction, RSXD at the Ni $L_{2,3}$ edges, and resonant x-ray diffraction (RXD) at the K threshold as techniques.

A $\text{La}_{1.8}\text{Sr}_{0.2}\text{NiO}_4$ single crystal was grown at the University of Cologne using the traveling solvent method. The crystalline quality was checked by x-ray diffraction and was found to be very good with a rocking width of 0.01° (FWHM) of the (204) reflection observed using resonant x-ray diffraction at the Ni- K -edge. Two pieces were cut and polished, one with a (101) surface orientation and one with (103). We refer to the commonly used orthorhombic unit cell with $a \approx b = 5.38 \text{ \AA}$ and $c = 12.55 \text{ \AA}$ (space group $Fmmm$). In this setting the direction of modulation of the electronic state in the NiO_2

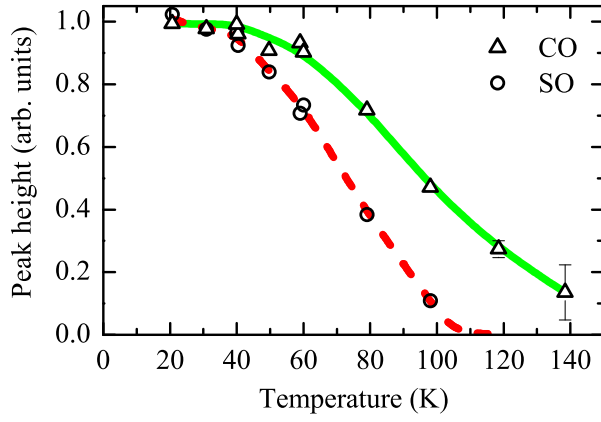


FIG. 1: (Color online) Temperature dependence of the peak height of the $(4 - 2\epsilon, 0, 1)$ charge-order peak (triangles) and $(1 - \epsilon, 0, 1)$ spin-order peak (circles) as probed by elastic neutron diffraction. The lines are guides to the eyes.

planes is along a and the stripes extend along b . Because of twinning, domains with the stripe pattern rotated by 90 degrees around c exist as well.

Neutron diffraction experiments were carried out at the Orphée reactor, diffractometer 3T.1 using a larger piece of the same single crystal. We probed the elastic signal from the $(1 - \epsilon, 0, 1)$ spin order and $(4 - 2\epsilon, 0, 1)$ charge order peaks with ϵ being the incommensurability parameter describing the spacing between stripes. The temperature dependence of the heights of both peaks is presented in Fig. 1. We found that the elastic magnetic signal (circles) decays at about 105 K while the elastic charge-order signal (triangles) is still visible at 140 K. The behavior of the two signals is very similar to the one Sachan *et al.* found for the elastic signals from their sample [Fig. 2(a) of Ref. 12].

The RSXD experiments were performed from the (101) sample at the soft x-ray beamlines U49/2-PGM1 and UE52-SGM of BESSY, using the two-circle UHV diffractometer, designed at the Freie Universität Berlin. The scattering geometry and sample orientation is described in Ref. 17. The photon polarization was linear and could be switched from parallel to the diffraction plane (π -polarization) to perpendicular (σ). RXD experiments at the Ni- K ($1s \rightarrow 4p$) threshold at 8358 eV were performed from the (103) sample at the MAGS-beamline at BESSY.

At the Ni ($2p \rightarrow 3d$) ($L_{2,3}$) resonance in the soft x-ray range, we probed the $(2\epsilon, 0, 1)$ charge order and the $(1 - \epsilon, 0, 0)$ spin order peak, which, for the chosen doping level, are both in the momentum space reachable at this photon energy (see Fig. 2). At the Ni ($1s \rightarrow 4p$) (K) resonance we probed the charge order at $\vec{q} = (2 - 2\epsilon, 0, 3)$.

As a measure of the intensity of the charge and spin order peaks we took the height of the maximum of the L_3 resonance¹⁷ in a photon energy dependent scan with the momentum transfer fixed at the corresponding peak position [see Fig. 2(c)]. The obtained temperature dependence of the CO signal is presented in Fig. 3(a). The

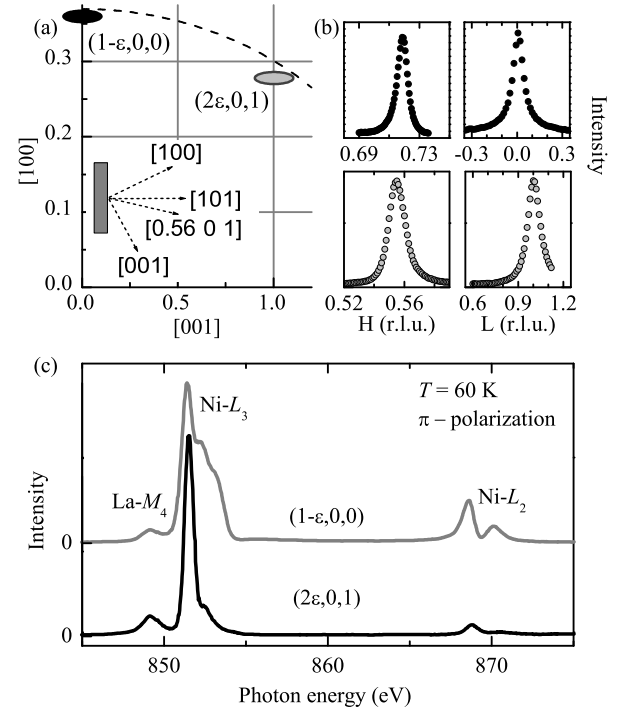


FIG. 2: (a) Position of the investigated superstructure peaks in k-space and (b) scans along the H- and L-direction (right) recorded at the Ni $L_{2,3}$ resonance with π -polarized light. Black symbol: $(1 - \epsilon, 0, 0)$ - spin order peak, gray symbol: $(2\epsilon, 0, 1)$ - charge order peak. The dashed line in panel (a) denotes the maximum possible momentum transfer at the Fe L_3 resonance. The inset shows the crystal directions in the scattering plane of the soft x-ray experiment. (c) Resonance spectra from the two peaks recorded with π -polarized light in the region of the $La-M_4$ and Ni- L_3 and L_2 resonances.

σ signal is about 50 percent higher than the π signal; for comparison the data were normalized to the value at 60 K. The effect of polarization on the temperature dependence is weak, both curves almost match. The corresponding data for the SO signal in Fig. 3(b) were normalized in the same way. The deviation between the SO temperature dependence observed with the two light polarizations can be attributed to the variation of the canting angle between the Ni spins and the b direction. In our scattering geometry with the detector at $\omega = 152^\circ$ we are probing with σ -polarized light essentially the projection of the spins on the a direction, while with π polarized light we are sensitive to the a and b components of the spin, the b component weighted by a factor $\sin^2 \omega = 0.22$. If we assume the spins to be confined to the ab plane^{10,24} we find a temperature-dependent canting angle as plotted in Fig. 3(c). The overall behavior of the spin direction is in agreement with results found for other doping levels.^{10,25,26}

From the intensity of the magnetic signal in the two polarization channels we can determine the *total* spin signal. This is plotted as the open symbols in Fig. 3(d) in comparison with the (averaged) CO signal. Both signals

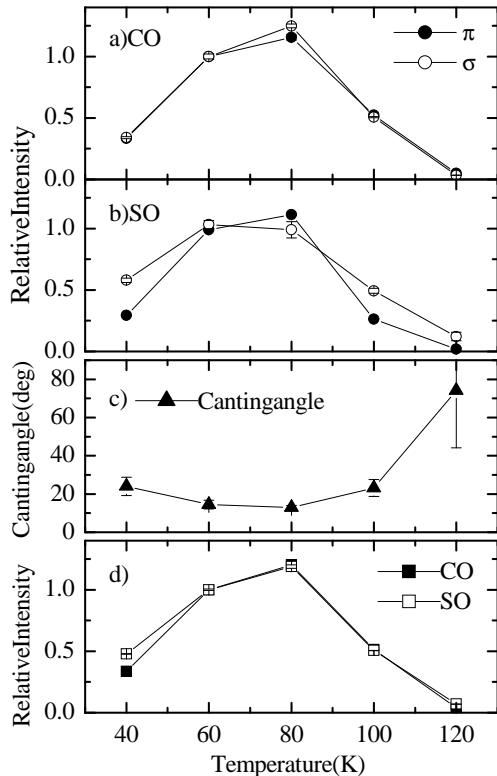


FIG. 3: Height of the maximum of the L_3 resonance above background vs. temperature for a) the charge-order signal and b) the spin-order signal. c) Canting angle as determined from the relative intensity of the spin-order signals. d) Average of the CO signals from a) compared to the total magnetic moment determined from the two SO curves. For comparison the curves in a), b), and c) have been normalized at 60 K. The lines are guides to the eye.

clearly have a very similar temperature dependence in particular above 60 K. This finding is very different from the neutron results presented in Fig. 1.

In Fig. 4 we compare in more detail the temperature dependences found in the neutron experiment (thick lines) with the ones from Fig 3(d). Focusing first on the higher temperatures, both RSXD signals appear to decay on a temperature scale that is in between those found by neutron diffraction for CO and SO. Particularly dramatic are the deviations between neutron and RSXD results at low temperatures: While both neutron signals increase upon cooling and eventually saturate, the RSXD signals decay upon cooling below 80 K. This kind of different temperature dependence is in agreement with what has been observed before using neutron^{6,7,8,10,12,18} and conventional x-ray diffraction,^{19,20,21,22,23} respectively.

In order to better characterize the temperature dependence we recorded the RSXD data in a second more dense data set. We used π -polarized light to probe the peak profile at the resonance maximum using scans along H and L (Fig. 5). The temperature dependence of the peak height as shown in Fig. 6(a) is very similar to the one

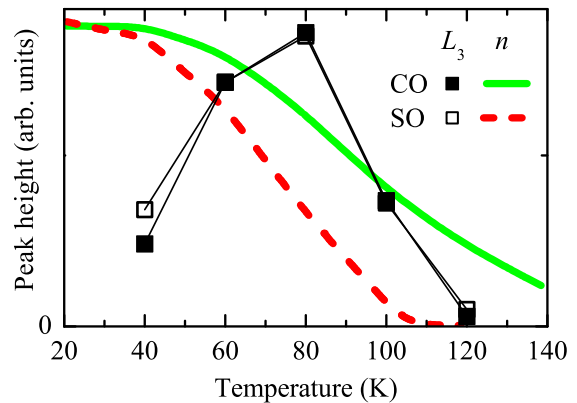


FIG. 4: (Color online) Comparison between neutron diffraction (thick lines) and the RSXD results (symbols and thin lines) for the temperature dependence of CO and SO.

in Fig. 3 with the maximum occurring at 70 K in this case. Again CO and SO signals behave similarly. We also show for comparison the CO signal as obtained at the Ni-K resonance (gray circles), which shows a temperature dependence very similar to the soft x-ray data.

As can be seen from the scans in Fig. 5 and from the extracted peak widths (assuming a Lorentzian line shape) in Fig. 6 (b) and (c), a decreasing peak height upon heating and cooling is accompanied by a broadening of the peak in both directions of reciprocal space. Consequently the integrated peak intensity is decaying much slower than the peak height. A similar trend of peak broadening is also found at the K -edge. We tried to estimate the integrated intensity from the L_3 data as the product of the peak height and peak widths in H and L directions. We can do this without double counting of intensities, because the q -space resolution broadening is about 10 times smaller than the smallest peak width in these two directions. Along the third, K , direction the intensity is mostly integrated because of the wide detector acceptance perpendicular to the scattering plane. The result of our estimate is shown in Fig. 6(d). In particular upon cooling the decrease of the peak heights seems to be fully compensated by the increasing peak widths. Upon heating the integrated intensity of the SO and CO signal stays almost constant up to 105 K. For higher temperatures the spin-order signal is difficult to track, because the temperature-dependent spin canting leads to an additional intensity loss for π -polarization [c.f. Fig. 3(b)]. The CO signal, however, is well observable and we find a gradual decay only at higher temperatures. We estimate the residual intensity at 135 K to 40 percent of the maximum intensity.

In a situation, where the peak height changes, but the integrated intensity is conserved, the detected signal depends strongly on the q -space resolution of the experiment. An experiment probing, e.g., CO, which is integrating over a wide range of q space, will rather find a temperature dependence as shown in Fig. 6(d): the signal

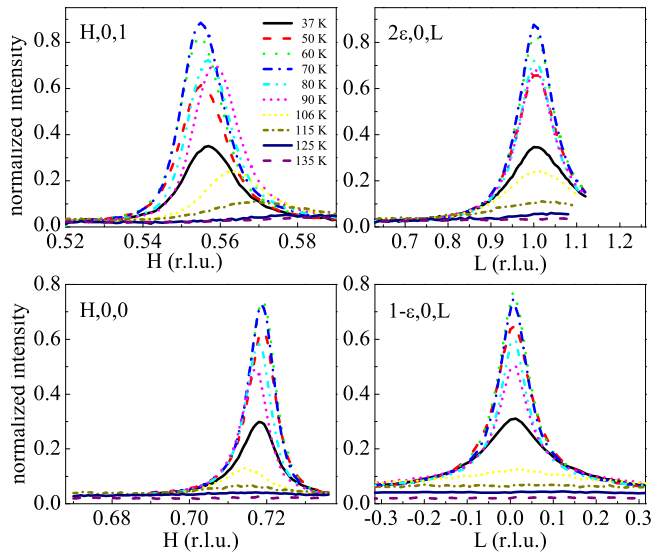


FIG. 5: (Color online) Scans through the superstructure peaks for different temperatures along H (left) and along L (right). Upper: charge order, lower: spin order.

is constant at low temperatures and decays slowly only at high temperatures. On the other hand, an experiment with high q -space resolution will mainly find a decrease of the peak height with decreasing temperature. Since neutron diffraction experiments are typically performed with lower resolution than x-ray diffraction experiments, this effect can at least partially explain the discrepancies between the low-temperature behavior found by neutron diffraction and x-ray diffraction from this system. The peak broadening can also explain, why the neutron CO signal in Fig. 4 appears to remain up to higher temperatures than the x-ray signal: the peak height probed in the x-ray experiments is decaying faster upon heating than the (partially) integrated intensity probed by neutron diffraction.

Having established the importance of the different q -space resolutions of the experiments, we are still left with the following observation: the temperature dependence of the charge and spin signals within the RSXD experiment is identical while it is very dissimilar in neutron diffraction. This observation cannot be attributed to differences in the q -space resolutions since the peak broadening effect applies to both the SO and CO signals with comparable widths as well. We need to look for another explanation. We infer that one has to look to the contribution from the *inelastic* magnetic scattering to the SO signal. For LSNO it is known, that the *total* magnetic scattering signal, i.e., the sum of elastic and inelastic magnetic neutron scattering has about the same temperature dependence as the CO signal.¹² The RSXD experiment was performed without energy analysis of the scattered photons. Unlike a neutron experiment, RSXD also lacks an intrinsic energy analysis.²⁷ In that sense RXSD is comparable to a hypothetical energy-integrated

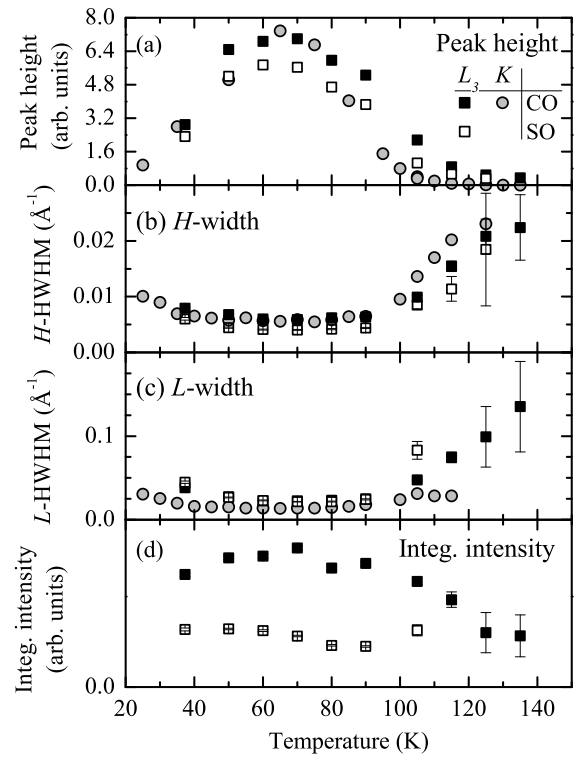


FIG. 6: Temperature dependence of the CO and SO peaks recorded at the Ni- L_3 resonance (filled and open squares) and of the CO peak recorded at the Ni- K resonance (gray circles): (a) peak height, (b) peak widths along H , (c) peak width along L , (d) integrated intensity estimated from the L_3 data.

neutron diffraction experiment,²⁸ and we have been probing the sum of static and fluctuating magnetic correlations.

To conclude, we studied the temperature dependence of SO and CO using RSXD, neutron diffraction and Ni- K -edge RXD for the CO signal. Differences in the q -space resolution of the different techniques have to be taken into account for a proper evaluation of diffraction intensities associated with the SO and CO superstructures. We find that in RSXD the SO and CO decay on the same temperature scale upon heating, very different from that in (elastic) neutron diffraction. The reason for this difference is that RSXD is probing the static and the fluctuating magnetic order and is hence in fact comparable to an energy-integrated neutron diffraction experiment. This in fact may open up an interesting experimental possibility to search for fluctuating order in other systems by comparing resonant soft x-ray diffraction and neutron diffraction data.

Acknowledgments

We gratefully acknowledge the expert support and excellent working conditions at BESSY and thank E. Weschke for making his UHV diffractometer available

for this work. We thank L. Hamdan and the mechanical workshop of the II. Physikalisches Institut in Cologne for their skillful technical assistance, and T. Koethe for help in preparing the experiment. Preliminary experiments were carried out at X1B of the NSLS and

we acknowledge experimental support by P. Abbamonte and A. Rusydi. The research in Köln is supported by the Deutsche Forschungsgemeinschaft through SFB 608. Work at BESSY was supported by the BMBF through project 05 ES3XBA/5.

* Corresponding author: schuessler@ph2.uni-koeln.de

- ¹ J. Zaanen and O. Gunnarsson, Phys. Rev. B **40**, 7391 (1989).
- ² V. J. Emery and S. A. Kivelson, Physica C **209**, 597 (19938).
- ³ J. M. Tranquada, B. J. Sternlieb, J. D. Axe, Y. Nakamura, and S. Uchida, Nature **375**, 561 (1995).
- ⁴ J. Orenstein and A. J. Millis, Science **288**, 468 (2000).
- ⁵ K. Yamada, C. H. Lee, K. Kurahashi, J. Wada, S. Wakimoto, S. Ueki, H. Kimura, Y. Endoh, S. Hosoya, G. Shirane, et al., Phys. Rev. B **57**, 6165 (1998).
- ⁶ J. M. Tranquada, J. E. Lorenzo, D. J. Buttrey, and V. Sachan, Phys. Rev. B **52**, 3581 (1995).
- ⁷ J. M. Tranquada, D. J. Buttrey, and V. Sachan, Phys. Rev. B **54**, 12318 (1996).
- ⁸ S.-H. Lee and S.-W. Cheong, Phys. Rev. Lett. **79**, 2514 (1997).
- ⁹ H. Yoshizawa, T. Kakeshita, R. Kajimoto, T. Tanabe, J. Katsufuji, and Y. Tokura, Phys. Rev. B **61**, R854 (2000).
- ¹⁰ D.-H. Lee, S.-W. Cheong, K. Yamada, and C. F. Majkrzak, Phys. Rev. B **63**, 060405 (2001).
- ¹¹ S.-H. Lee, J. M. Tranquada, K. Yamada, D. J. Buttrey, Q. Lin, and S.-W. Cheong, Phys. Rev. Lett. **88** (2002).
- ¹² V. Sachan, D. J. Buttrey, J. M. Tranquada, J. E. Lorenzo, and G. Shirane, Phys. Rev. B **51**, 12742 (1995).
- ¹³ P. Abbamonte, L. Venema, A. Rusydi, G. A. Sawatzky, G. Logvenov, and I. Bozovic, Science **297**, 581 (2002).
- ¹⁴ S. B. Wilkins, P. D. Spencer, P. D. Hatton, S. P. Collins, M. D. Roper, D. Prabhakaran, and A. T. Boothroyd, Phys. Rev. Lett. **91**, 167205 (2003).
- ¹⁵ S. S. Dhesi, A. Mirone, C. De Nadai, P. Ohresser, P. Benck, N. B. Brookes, P. Reutler, A. Revcolevschi, A. Tagliaferri, O. Toulemonde, et al., Phys. Rev. Lett. **92**, 056403 (2004).
- ¹⁶ K. J. Thomas, J. P. Hill, S. Grenier, Y.-J. Kim, P. Abbamonte, L. Venema, A. Rusydi, Y. Tomioka, Y. Tokura, D. F. McMorrow, et al., Phys. Rev. Lett. **92**, 237204 (2004).
- ¹⁷ C. Schüßler-Langeheine, J. Schlappa, A. Tanaka, Z. Hu, C. F. Chang, E. Schierle, M. Benomar, H. Ott, E. Weschke, G. Kaindl, et al., Phys. Rev. Lett. **95**, 156402 (2005).
- ¹⁸ S. M. Hayden, G. H. Lander, J. Zarestky, P. J. Brown, C. Stassis, P. Metcalf, and J. M. Honing, Phys. Rev. Lett. **68**, 1061 (1992).
- ¹⁹ C.-H. Du, M. E. Ghazi, Y. Su, I. Pape, P. D. Hatton, S. D. Brown, W. G. Stirling, M. J. Cooper, and S.-W. Cheong, Phys. Rev. Lett. **84**, 3911 (2000).
- ²⁰ P. D. Hatton, M. E. Ghazi, W. B. Wilkins, P. D. Spencer, D. Mannix, T. d'Almeida, P. Prabhakaran, A. Boothroyd, and C. W. Cheong, Physica B **318**, 289 (2002).
- ²¹ P. D. Hatton, M. E. Ghazi, W. B. Wilkins, P. D. Spencer, D. Mannix, T. d'Almeida, P. Prabhakaran, and A. Boothroyd, Int. J. Mod. Phys. B **16**, 1633 (2002).
- ²² M. E. Ghazi, P. D. Spencer, S. B. Wilkins, P. D. Hatton, D. Mannix, D. Prabhakaran, A. T. Boothroyd, and S.-W. Cheong, Phys. Rev. B **70**, 144507 (2004).
- ²³ P. D. Spencer, M. E. Ghazi, S. B. Wilkins, P. D. Hatton, S. D. Brown, D. Prabhakaran, and A. T. Boothroyd, Eur. Phys. J. B **46**, 27 (2005).
- ²⁴ G. Aeppli and D. J. Buttrey, Phys. Rev. Lett. **61** (1988).
- ²⁵ P. G. Freeman, A. T. Boothroyd, D. Prabhakaran, D. González, and M. Enderle, Phys. Rev. B **66**, 212405 (2002).
- ²⁶ P. G. Freeman, A. T. Boothroyd, D. Prabhakaran, M. Enderle, and C. Niedermayer, Phys. Rev. B **70**, 024413 (2004).
- ²⁷ In neutron scattering the energy of magnetic fluctuations of the order of 10 meV leads to a sizable change of the neutron momentum $k_{\text{Neutron}} \propto E_{\text{Neutron}}^{1/2}$ due to the small neutron energies, which are of the order of 50 meV. For soft x-rays with photon energies, E_{Photon} , of several 100 eV, such an energy change has only negligible influence on the photon wave vector, $k_{\text{Photon}} \propto E_{\text{Photon}}$.
- ²⁸ In general such an energy integrating neutron scattering experiment is not possible directly, because even without energy analyzer a neutron diffraction experiment does not integrate all the inelastic scattering for a given scattering vector \vec{q} . For layered materials like LSNO with two-dimensional magnetic fluctuations, however, one can set the direction of the outgoing neutron momentum parallel to the c^* -direction, i.e. perpendicular to the plane of magnetic correlations and in that way achieve an energy integration.